Multi-modal calculations of prompt fission neutrons from ^{238}U(n, f) at low induced energy*

ZHENG Na(郑娜) ZHONG Chun-Lai(钟春来) FAN Tie-Shuan(樊铁栓)[1)]

State Key Laboratory of Nuclear Physics and Nuclear Technology and School of Physics, Peking University, Beijing 100871, China

Abstract: Properties of prompt fission neutrons from ^{238}U(n, f) are calculated for incident neutron energies below 6 MeV using the multi-modal model, including the prompt fission neutron spectrum, the average prompt fission neutron multiplicity, and the prompt fission neutron multiplicity as a function of the fission fragment mass $\upsilon(A)$ (usually named "sawtooth" data) The three most dominant fission modes are taken into account. The model parameters are determined on the basis of experimental fission fragment data. The predicted results are in good agreement with the experimental data.

Key words: ^{238}U (n, f), fission, prompt neutron, multi-model, Los Alamos model

PACS: 25.85.Ec, 24.10.-i, 24.75.+i **DOI:** 10.1088/1674-1137/35/10/008

1 Introduction

With the development of extended burn-up of nuclear fuel and the design of accelerator-driven systems for the transmutation of nuclear waste [1], the need for accurate nuclear data has become more important. Prompt neutrons afford important information for understanding the fission process. Thus new calculations are required with a higher accuracy that can shed some light on the nuclear fission process itself. [2].

In the calculations of prompt fission neutron energy spectrum and multiplicity of actinides, some important approaches, the Maxwellian, Watt spectrum [3], Los Alamos (LA) model [4, 5], the Dresden model [6] and the Hauser-Feshbach statistical model [7] have been developed. The LA model, which has good predictive power with fewer input parameters, is widely used. Based on the LA model, the "point by point" model [8, 9] (PBP) is expanded to calculate prompt fission neutrons as a function of the fission fragment mass.

For low-energy fission of actinide nuclei, the experimental data from fragment mass distributions show that multi-modal fission is the most promising model [10, 11]. The many calculations performed by Brosa [12], Schillebeeckx [13], Fan [14, 15], Dematte [16] and Ohsawa [17] et al., have shown that multi-modal analysis is successful for both understanding the low-energy fission process and predicting the fission fragment properties.

Neutrons from the newborn fission fragments constitute the majority of the prompt neutrons. Thus the prompt neutron properties are dependent on the fission modes. For neutron-induced fission of actinides, multi-modal analysis of the prompt neutron spectrum and the multiplicity is necessary and has been applied successfully to calculation of the prompt neutron spectrum of actinide isotopes by Ohsawa [18–20], Hambsch [21–23], Vladuca [24] and Zheng [25, 26] et al.

In this paper, a new attempt is made to improve the evaluation of the prompt fission neutron spectrum, the average prompt fission neutron multiplicity and the prompt fission neutron multiplicity as functions of the fragment mass $\upsilon(A)$ from ^{238}U(n, f) for incident neutron energy below 6 MeV, using multi-modal analysis in the calculation of $\upsilon(A)$ for the first time. The prompt fission neutrons are calculated in the framework of the multi-modal approach. The

Received 28 December 2010

* Supported by State Key Development Program for Basic Research of China (2008CB717803, 2009GB107001, 2007CB209903) and Research Fund for the Doctoral Program of Higher Education of China (200610011023)

1) Corresponding author. E-mail: tsfan@pku.edu.cn

three main fission modes, two asymmetric modes named standard I (S1) and standard (S2), and one symmetric mode named superlong (SL), are taken into account. The partial spectrum, multiplicity, and $\upsilon(A)$ of each mode (Sl, S2 and SL) are calculated separately by the improved LA [5] and PBP models [9]; the totals are compared with the experimental data.

2 Methods

2.1 Basic features

In the framework of multi-modal fission, the prompt fission neutron spectrum $N(E)$, the average prompt fission neutron multiplicity $\upsilon_{\rm p}$, and the "sawtooth" multiplicity $\upsilon(A)$ are calculated by the superposition of the corresponding quantities associated with a particular fission mode, respectively, by:

$$N(E) = \frac{\sum_m \omega_m \langle\upsilon\rangle_m N_m(E)}{\sum_m \omega_m \langle\upsilon\rangle_m}, \quad (1)$$

$$\upsilon_{\rm p} = \frac{\sum_m \omega_m \langle\upsilon\rangle_m}{\sum_m \omega_m}, \quad (2)$$

$$\upsilon(A)^{\rm pair} = \frac{\sum_m \omega_m \upsilon(A)^{\rm pair}_m}{\sum_m \omega_m}. \quad (3)$$

In Eqs. (1), (2) and (3), ω_m is the branching ratio of mode m. The quantities $N_m(E)$, $\langle\upsilon\rangle_m$ and $\upsilon(A)^{\rm pair}_m$ are the prompt fission neutron spectrum, average prompt fission neutron multiplicity and "sawtooth" multiplicity for mode m, respectively. The prompt neutron spectrum $N_m(E)$ and average prompt fission neutron multiplicity $\langle\upsilon\rangle_m$ are obtained from Weisskopf evaporation theory [27] and energy conservation, and the detailed procedures can be found in Refs. [5] and [25].

The prompt neutron multiplicity of each FF pair (indexed i) of each mode is given by

$$\upsilon^{\rm pair}_{i,m} = \frac{TXE_{im} - q}{S_{{\rm n},im} + \langle\varepsilon\rangle_m + p}, \quad (4)$$

where $\upsilon(A)^{\rm pair}_m$is given by the sum of the multiplicity for neutron emission from the light fragment L and from the heavy fragment H

$$\upsilon^{\rm pair}_{i,m} = \upsilon^{\rm L}_{i,m} + \upsilon^{\rm H}_{i,m}, \quad (5)$$

and TXE is the excitation energy of the i-th FFs, given by

$$TXE_{im} = E_{r,im} + E_{\rm n} + B_{\rm n} - TKE_{im}, \quad (6)$$

$$TXE^*_{{\rm L}i} = \frac{A_{{\rm L}i}}{A} TXE^*_i \quad TXE^*_{{\rm H}i} = \frac{A_{{\rm H}i}}{A} TXE^*_i, \quad (7)$$

where $E_{r,im}$ is the energy released to produce the i-th FFs for the mode m, $E_{\rm n}$ is the incident neutron energy, $B_{\rm n}$ is the neutron separation energy of the compound nucleus ^{239}U, and TKE_{im} is the kinetic energy of the i-th FFs.

$S_{{\rm n},im}$ is the neutron separation energy from the i-th FF, and $\langle\varepsilon\rangle_m$ is the first-order moment of the center-of-mass system spectrum of each mode, and the P and q are parameters corresponding to the compound nucleus [28]:

$$p = 6.71 - 0.156\frac{Z^2_{\rm CN}}{A_{\rm CN}}, \quad q = 0.750 + 0.088\frac{Z^2_{\rm CN}}{A_{\rm CN}}. \quad (8)$$

In the prompt fission neutron calculation, the parameters include the average energy released, the average neutron separation energy from the FFs, the average total kinetic energy of the FFs, and the level density parameter. For incident neutron energies below (n, nf) thresholds, multi-modal calculations of prompt fission neutron are implemented by multi-modal calculation of these parameters, and the method is discussed in the following section.

2.2 Multi-modal parameter calculation

The parameters of the LA model are calculated multi-modally for ^{238}U for incident neutron energy below 6 MeV, including the average energy released for each fission mode, the average neutron separation energy from the FFs for each fission mode, the average total kinetic energy of the FFs for each fission mode, as well as multi-modal calculation of the level density parameter.

A systematic multi-modal analysis of the experimental data [29] of the fragment mass distributions for ^{238}U (n, f) is performed, and the experimental FF mass ranges $A_{\rm L} \in [63, 119]$ and $A_{\rm H} \in [120, 176]$ are taken into account, a few spread experimental distribution points corresponding to far asymmetric FF mass pairs being neglected. The experimental data are analyzed to determine multi-modal branching ratios ω_m. For each FF mass pair, four isobars per mass are taken into account with values of the nuclear charge Z which are the nearest integer values above and below the most probable charge.

Calculations of the LA model parameters have been processed for other actinide isotopes; the details can be seen in Ref. [25]. In the present paper, we just show the main multi-modal results of the fission fragment mass distribution, the kinetic energy distribution, and the procedure of the multi-modal calculation of the level density parameter, not considered in our previous work.

Comparisons between the calculated results and the experimental data for ^{238}U (n, f) at $E_{\rm n}$ = 1.8, 3.0, 4.5, 5.8 MeV are shown in Fig. 1, where

it can be seen that the multi-modal calculation can reproduce the experimental data, the branching ratio of SL mode increases with incident neutron energy, and the positions of the S1 and S2 models are invariable, corresponding to the shell effect.

The calculated values of the average total kinetic energy $TKE(A)$ of the FFs from ^{238}U (n, f) at $E_{\rm n}$=3.0 MeV are plotted versus heavy fragment mass in Fig. 2(a). It is evident from this figure that there are some differences between the calculated and experimental data, whereas the difference of average total kinetic energy between them is within 0.5% as shown in Fig. 2(b).

Unlike previous calculations, the present work considers the multi-modal calculation of the level density parameter. The average value of the level density parameter for each fission mode m is calculated as

$$\langle a\rangle_m = \frac{\sum\limits_i Y_{mi} \sum\limits_{j=z_{\rm p}-2}^{j=z_{\rm p}+2} pz_{i,j}a_{i,j}}{\sum\limits_i Y_{mi} \sum\limits_{j=z_{\rm p}-2}^{j=z_{\rm p}+2} pz_{i,j}}, \tag{9}$$

where m is the index of the mode (S1, S2, SL), i is the range of FF pairs, Y_{mi} is the FF mass yield for mode m and FF pair i, and pz_i is the charge distribution corresponding to the FF pair i, approximated by a Gaussian function [30]. The full width at half maximum (FWFM) of the Gaussian function is 0.25. $a_{i,j}$ is the level density parameter of each FF, calculated using the back-shifted Fermi gas model [31, 32]. The dependence of $\langle a\rangle_m$ on the incident neutron energy $E_{\rm n}$ is plotted in Fig. 3.

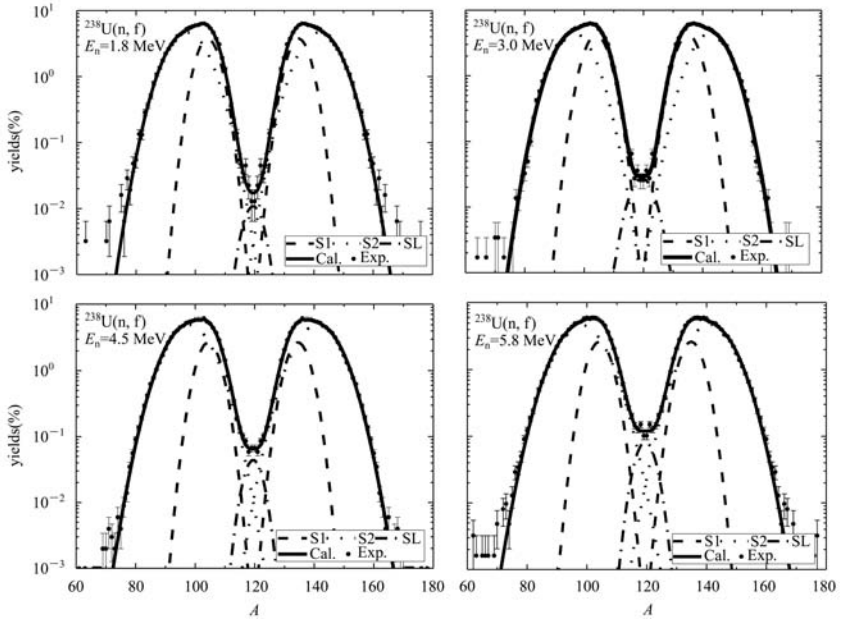

Fig. 1. Mass distributions of fission fragments for ^{238}U(n, f) for incident neutron energies of 1.8, 3.0, 4.5, 5.8 MeV. The contributions of fission modes are shown with dashed (for S1 mode), dotted (for S1 mode), and dash-dotted (for SL mode) lines. The solid curves show the superposition results of the three modes. The experimental data [29] are shown with solid circles.

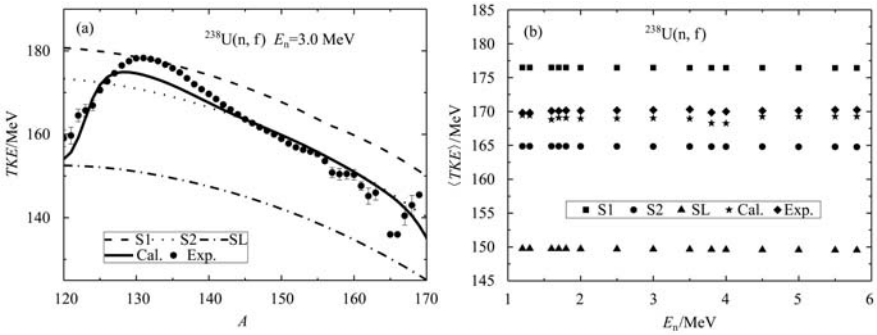

Fig. 2. (a) Comparison of experimental data [29] with the corresponding fit of the $TKE(A)$ for ^{238}U (n, f) at $E_{\rm n}$=3.0 MeV, (b) Calculated average total kinetic energy $\langle TKE\rangle$ of the fragments from ^{235}U(n, f) for the S1, S2 and SL modes as a function of the incident neutron energy, and comparison between the calculated and experimental data [29].

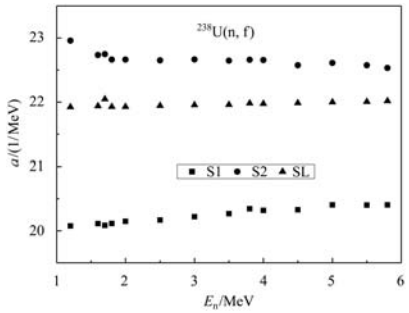

Fig. 3. Average value of the level density parameter for the S1, S2 and SL modes as a function of the incident neutron energy for ^{238}U(n, f).

3 Results and discussion

3.1 Multi-modal calculation of the prompt fission neutron spectrum

In the present work, the prompt fission neutron spectra of ^{238}U(n, f) for incident energies below 6.0 MeV are calculated in the framework of the multi-modal LA modal. The calculation shows that the larger the deformation of the compound nucleus, the harder its corresponding spectrum will be. These results agree with the experimental observation and previous calculations.

The present multi-modal calculation results of prompt fission neutron spectra from ^{238}U(n, f) for $E_n = 2.0$ MeV, the multi-modal calculation of Hambach [21], and the experimental data are shown in Fig. 4. It shows that the multi-modal calculations agree well with the experimental data [33]. There is some difference between the two calculated results, and the difference is from the different multi-modal analysis of the FFs mass distributions.

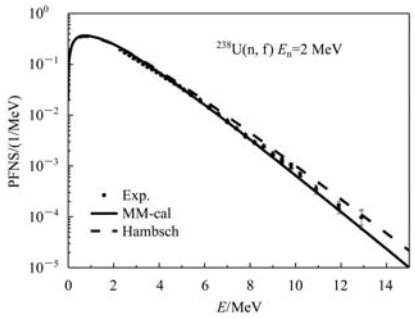

Fig. 4. Comparison of the calculated total neutron spectra with the experimental data [33] and the multi-modal calculation of Hambach [21] for 2 MeV neutron induced fission of ^{238}U.

The multi-modal calculation results of prompt fission neutron spectra of ^{238}U(n, f) for $E_n = 2.9$ MeV are shown in Fig. 5(a), along with the experimental data [34] and single modal calculation results. There is an obvious difference between two calculation results, and the multi-modal calculation can reproduce the experiment result much better. The present calculated prompt fission neutron spectrum ratio to ^{252}Cf spontaneous fission spectrum at $E_n = 2.9$ MeV, and the experimental data are shown in Fig. 5(b). It shows that the two results are not as coincident as in Fig. 5(a). The main reason may be due to the data of the standard spectrum.

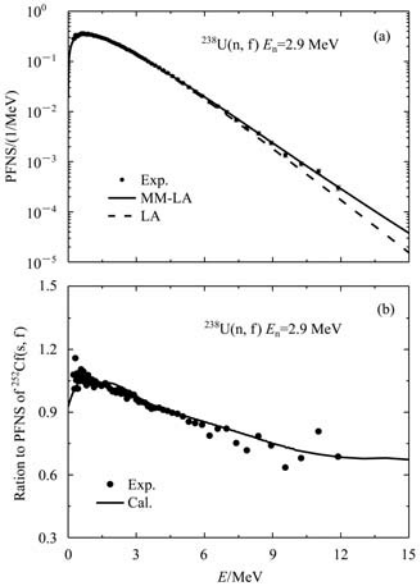

Fig. 5. Comparison of the multi-modal LA model calculated prompt neutron spectrum of ^{238}U (n, f) at $E_n = 2.9$ MeV with (a) the original LA modal calculation and experimental data [34]; (b) the prompt fission neutron spectrum of the ^{252}Cf (s, f) spectrum used as a reference.

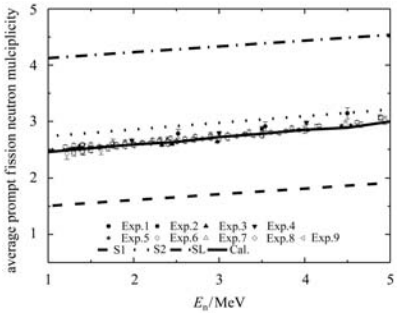

Fig. 6. Average prompt fission neutron multiplicity (solid line) as a function of incident neutron energy, compared with the experimental data [35], and the contributions of the three fission modes are also shown.

The multi-modal calculation of average prompt fission neutron multiplicity (PFNM) for incident neutrons below the (n, nf) threshold and the experimental data [35] are shown in Fig. 6. The partial prompt

fission neutron multiplicity of fission modes S1, S2 and SL are also given in Fig. 6.

The prompt fission neutron multiplicity as function of the fission fragment mass $\upsilon(A)$ is calculated from Eqs. (3)–(7) in the framework of the multi-modal approach.

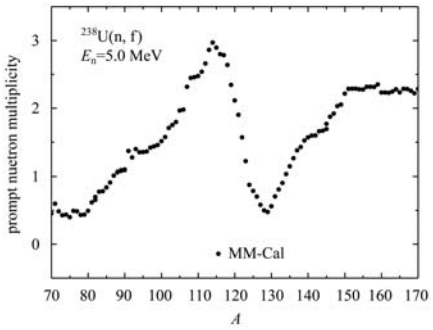

Fig. 7. Multi-modal calculation of the prompt fission neutron multiplicity as a function of the fragment mass for ^{238}U (n, f) for $E_{\rm n}$=5 MeV.

Because the experimental data of $\upsilon(A)$ for ^{238}U(n, f) are scarce and unavailable, the present paper just shows the results of multi-modal calculations in Fig. 7.

4 Conclusions

The Los Alamos model and the point-by-point model in the framework of the multi-modal approach are used to calculate the prompt fission neutron properties from ^{238}U(n, f) for incident neutrons below 6 MeV. The present calculation is on the basis of multi-modal analysis of the FFs mass distributions. Compared with the original LA calculation, the multi-modal calculation of the prompt fission neutron spectrum is in better agreement with the experimental data. The multi-modal calculation of the average prompt fission neutron multiplicity can reproduce the experimental data well. The present calculation of the prompt fission neutron multiplicity as function of FFs mass $\upsilon(A)$ can be used as reference. The method of prompt fission neutron calculation has many useful applications.

References

1 Kerdraon D, Billebaud A, Brissot R et al. Prog. Nucl. Energy, 2003, **42**(1): 11
2 Kornilov N V, Hambsch F J, Fabry I. In Proceedings of the International Conference on Nuclear Data for Science and Technology. Bern: EPD Science, 2007. 387
3 Terrell J. Phys. Rev., 1959, **113**(2): 527
4 Madland D G, Nix J R. Nucl. Sci. Eng., 1982, **81**(2): 213
5 Vladuca G, Tudora A. Computer Physics Communications, 2000, **125**(1–3): 221
6 Marten H, Ruben A, Seeliger D. IAEA-INDC (NDS), 1989, **220**: 245
7 Browne J C, Dietrich F S. Phys. Rev. C, 1974, **10**(6): 2545
8 Madland D G, LaBauve R J, Nix J R. IAEA-INDC(NDS), 1989, **220**: 259
9 Tudora A, Morillon B, Hambsch F J et al. Nucl. Phys. A, 2005, **756**(1–2): 176
10 WANG Fu-Cheng, HU Ji-Min. J Phys. G: Nucl. Part. Phys., 1989, **15**(6): 829
11 Knitter H H, Hambsch F J, Jorgensen C B et al. Z. Naturf., 1987, **42a**: 786
12 Brosa U, Grossmann S, Muller A. Phys. Rep., 1990, **197**(4): 167
13 Schillebeeckx P, Wagemans C, Deruytter A et al. Nucl. Phys. A, 1992, **545**(3): 623
14 FAN T S, HU J M, BAO S L. Nucl. Phys. A, 1995, **591**(2): 161
15 FAN T S, HU J M, BAO S L. HEP&NP, 1996, **20**(2): 187 (in Chinese)
16 Demattè L, Wagemans C, Barthéléy R et al. Nucl. Phys. A,1997, **617**(3): 331
17 Ohsava T, Hayashi H, Ohtani Y. In Proceedings of the International Conference on Nuclear Data for Science and Technology, ICTP Trieste, Italy. (Italian Physical Society, Bologna), 1997. 365
18 Ohsawa T, Horiguchi T, Hayashi H. Nucl. Phys. A, 1999, **653**(1): 17
19 Ohsawa T, Horiguchi T, Mitsuhashi M. Nucl. Phys. A, 2000, **665**(1): 3
20 Ohsawa T J. Nucl. Radiochem. Sci., 2002, **3**(1): 93
21 Hambsch F J, Oberstedt S, Vladuca G et al. Nucl. Phys. A, 2002, **709**(1–4): 85
22 Hambsch F J, Oberstedt S, Tudora A et al. Nucl. Phys. A, 2003, **726**(3–4): 248
23 Hambsch F J, Tudora A, Vladuca G et al. Annals of Nuclear Energy, 2005, **32**(10): 1032
24 Vladuca G, Tudora A. Annals of Nuclear Energy, 2001, **28**(16): 1643
25 ZHENG N, DING Y, ZHONG C L et al. Chin. Phys. B, 2009, **18**(4): 1
26 ZHENG N, FAN T S, DING Y et al. Chin. Phys. C (HEP & NP), 2010, **34**(1): 49
27 Weisskopf V F. Rev. Mod. Phys., 1957, **29**(2): 174
28 Frehaut J. IAEA INDC (NDS), 1989, **220**: 99
29 Vives F, Hambsch F J, Bax H et al. Nucl. Phys. A, 2000, **662**(1–3): 63
30 Reisdorf W, Unik J P, Griffin H C et al. Nucl. Phys. A, 1971, **177**(2): 337
31 Dilg W, Schantl W, Vonach H. Nucl. Phys. A, 1973, **217**(2): 269
32 Plyaskin V I, Kosilov R A. Physics of Atomic Nuclei, 2000, **63**(5): 752
33 Baba M, Wakabayashi H, Ishikawa M et al. IAEA-INDC (NDS),1989, **220**: 149
34 Boykov G S, Dmitriev V D, Kudyaev G A et al. Annals of Nuclear Energy, 1994, **21**(10): 585
35 www-nds.iaea.org/exfor/, Experimental Nuclear Reaction Data (EXFOR) Database (2010), entry numbers: 14215003, 20075002, 20490002, 21135006, 23054006, 32606002,40342002, 40429003, 40665002